Sodium Hydrazinidoborane: A Chemical Hydrogen-Storage Material

Romain Moury,[a] Umit B. Demirci,*[a] Takayuki Ichikawa,[b] Yaroslav Filinchuk,[c] Rodica Chiriac,[d] Arie van der Lee,[a] and Philippe Miele[a]

Herein, we present the successful synthesis and full characterization (by [11]B magic-angle-spinning nuclear magnetic resonance spectroscopy, infrared spectroscopy, powder X-ray diffraction) of sodium hydrazinidoborane ($NaN_2H_3BH_3$, with a hydrogen content of 8.85 wt%), a new material for chemical hydrogen storage. Using lab-prepared pure hydrazine borane ($N_2H_4BH_3$) and commercial sodium hydride as precursors, sodium hydrazinidoborane was synthesized by ball-milling at low temperature ($-30\,°C$) under an argon atmosphere. Its thermal stability was assessed by thermogravimetric analysis and differential scanning calorimetry. It was found that under heating sodium hydrazinidoborane starts to liberate hydrogen below $60\,°C$. Within the range of $60–150\,°C$, the overall mass loss is as high as 7.6 wt%. Relative to the parent $N_2H_4BH_3$, sodium hydrazinidoborane shows improved dehydrogenation properties, further confirmed by dehydrogenation experiments under prolonged heating at constant temperatures of 80, 90, 95, 100, and $110\,°C$. Hence, sodium hydrazinidoborane appears to be more suitable for chemical hydrogen storage than $N_2H_4BH_3$.

Introduction

Among the boranes considered for chemical hydrogen storage,[1] hydrazine borane ($N_2H_4BH_3$) is one of the most recent materials.[2] Remarkably, hydrazine borane (HB) presents four protic hydrogen atoms ($H^{\delta+}$), in tandem with three hydridic hydrogen atoms ($H^{\delta-}$). Therefore, it presents material-based[3] gravimetric and volumetric hydrogen-storage capacities as high as 15.4 wt% and 146 g L^{-1}, respectively. Another beneficial feature is that pure HB is stable at ambient conditions, when stored under an argon atmosphere.[4] It is also stable in degassed aqueous solutions over a few weeks.[5] Therefore, the challenge has been to dehydrogenate HB to a large degree under ambient/mild conditions (i.e., at $\leq 85\,°C$ and atmospheric pressure, which are criteria for on-board hydrogen-storage systems for light-duty vehicles).[6]

HB can be considered as a derivative of ammonia borane (NH_3BH_3), in which the NH_3 moiety has been replaced by N_2H_4. NH_3BH_3 has attracted a lot of attention in thermolytic dehydrogenation contexts within the past decade, but the first attempts at its thermolysis date back to the 1970–80s.[7] NH_3BH_3 dehydrogenates at temperatures higher than $100\,°C$, releasing H_2 and byproducts, such as the unwanted borazine and diborane, and leading to a solid residue (BNH_x).[8] The dehydrogenation of HB, similarly to NH_3BH_3,[9] can be initiated by adding a metal-based catalyst (e.g., nickel-based bimetallic alloys) into the aqueous solution at low temperatures,[5,10] or by heating the solid under an inert atmosphere.[4,11] Through the first approach, the catalytic dehydrogenation of HB takes place according to a two-step reaction that consists of both the hydrolysis of the BH_3 group and the decomposition of the N_2H_4 moiety. This approach presents the advantage of occurring at relatively low temperatures ($50\,°C$).[10] However, thermolytic dehydrogenation may be more attractive due to the fact that the reaction is easily performed by heating the borane only.

The thermolytic dehydrogenation of HB initiates at $60\,°C$, simultaneously with HB melting, revealing an endothermic peak with an enthalpy of 15 kJ mol^{-1} in the differential scanning calorimetry (DSC) curve. A mass loss of 1.2 wt% at $95\,°C$, as determined by thermogravimetric analysis (TGA) at a heating rate of $1\,°C\,min^{-1}$ was reported.[12] A second mass loss of 28.7 wt% occurs within $105–160\,°C$ due to the release of N_2H_4. A third mass loss of 4.3 wt% is observed at about $250\,°C$. In this way, 2 equiv of H_2 are released and a shock-sensitive solid residue forms.[12] The high dehydrogenation temperatures and the formation of hazardous byproducts are significant problems, making HB unsuitable for mobile and portable hydrogen storage. Consequently, strategies have been recently adopted to

[a] R. Moury, Dr. U. B. Demirci, Dr. A. van der Lee, Prof. P. Miele
IEM (Institut Europeen des Membranes)
UMR 5635 (CNRS-ENSCM-UM2), Universite Montpellier 2
Place E. Bataillon, 34095, Montpellier (France)
Fax: (+33) 04-67-14-91-19
E-mail: umit.demirci@um2.fr

[b] Dr. T. Ichikawa
Institute for Advanced Materials Research
Hiroshima University
1-3-1 Kagamiyama, Higashi-Hiroshima, 739-8530 (Japan)

[c] Prof. Y. Filinchuk
Institute of Condensed Matter and Nanosciences
Université Catholique de Louvain
Place L. Pasteur 1, 1348 Louvain-la-Neuve (Belgium)

[d] Dr. R. Chiriac
Laboratoire des Multimatériaux et Interfaces
Université Lyon 1, CNRS, UMR 5615
43 Boulevard du 11 Novembre 1918, 69622 Villeurbanne (France)

Supporting Information for this article is available on the WWW under
http://dx.doi.org/10.1002/cssc.201200800.

improve the dehydrogenation properties of HB and avoid the evolution of unwanted gaseous and solid byproducts. The first strategy involves mixing HB with LiH[11] and the second chemical modification of HB by replacing one $H^{\delta+}$ atom by an alkaline cation, such as Li$^+$, which leads to the formation of LiN$_2$H$_3$BH$_3$.[13]

In view of the issues encountered in HB thermolysis, we decided to follow (right after our work dedicated to this borane)[12] the chemical modification approach. We then started to work on the elaboration of metal hydrazinidoboranes (MN$_2$H$_3$BH$_3$, M = Li or Na), which attractively show parity in protic and hydridic hydrogen atoms (three $H^{\delta+}$ and three $H^{\delta-}$ atoms, whereas metal amidoboranes have just two $H^{\delta+}$ for three $H^{\delta-}$ atoms). Herein, we report for the first time the successful synthesis and characterization of NaN$_2$H$_3$BH$_3$ (NaHB).

Results and Discussion

Solubility and stability of NaHB

Sodium hydrazinidoborane (hydrogen content of 8.85 wt%) is a colorless solid, paste-like at 3–4 °C, but powdery at 20 °C. It is insoluble in common organic solvents, such as THF and toluene, but reacts with water or methanol (i.e., hydrolysis and methanolysis of the BH$_3$ moiety; see the Supporting Information, Figure S1). For stability reasons, it has to be stored under an argon atmosphere.

Molecular structure of NaHB

The molecular structure of NaHB was analyzed by solid-state ^{11}B magic-angle-spinning (MAS) NMR spectroscopy. The spectrum was compared to that of HB (Figure 1). Both samples have a single NBH$_3$ environment. Unlike HB, displaying a split signal due to a quadrupolar coupling centered at −23.2 ppm, NaHB shows a single symmetric resonance at −16.5 ppm, suggesting isotropy around the boron atom and a higher molecular degree of freedom. This indicates a different destabilized $H^{\delta+}\cdots H^{\delta-}$ network relative to that found in HB. The signal is
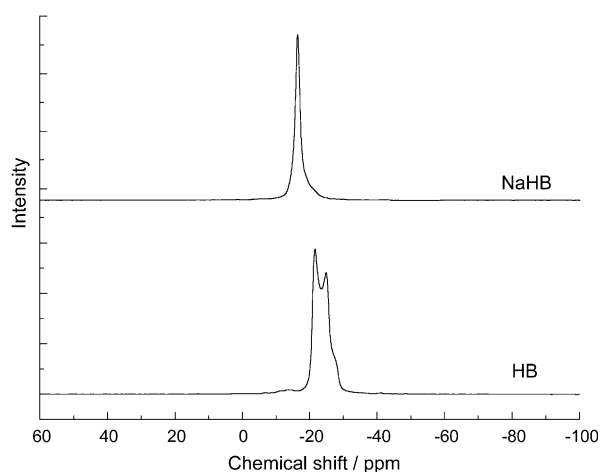
Figure 1. ^{11}B MAS NMR spectra of NaHB and HB.

sharp, which is characteristic of high crystallinity. The difference in the chemical shifts is consistent with a change of the chemical environment of B in NaHB.

Analysis by IR spectroscopy (Figure 2) showed slight changes relative to HB. The changes are mainly visible for the N–H stretching (2600–3600 cm^{-1}), bending (1800–1300 cm^{-1}), and rocking (1100–900 cm^{-1}) regions. The bands shown by NaHB
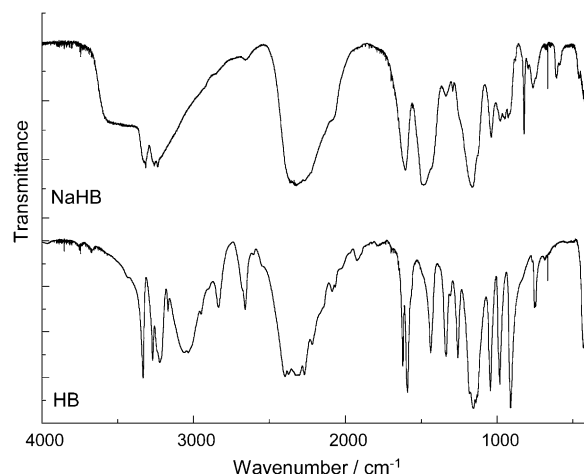
Figure 2. IR spectra of NaHB and HB with: N–H stretching at 2600–3600 cm^{-1}, B–H stretching at 2000–2600 cm^{-1}, N–H bending (also B–N stretching) at 1300–1800 cm^{-1}, B–H bending at 1100–1300 cm^{-1}, N–H rocking at 900–1100 cm^{-1}, and BN–N stretching at 600–900 cm^{-1}.

are either broadened or weakened, consistent with the change of the environment of the N–H bonds by the introduction of Na$^+$. The B–H bonds display large and strong bands in the stretching (2000–2600 cm^{-1}) and bending regions (1100–1300 cm^{-1}). With respect to the B–N bond, several bands in the BN–N asymmetric and symmetric stretching regions (600–900 cm^{-1}) are observed.

Crystal structure of NaHB

NaHB was analyzed by powder XRD. Figure 3 shows an XRD pattern of single-phase NaN$_2$H$_3$BH$_3$ and its comparison with patterns of the starting compounds. Diffraction data were indexed in a monoclinic unit cell. The systematic absences suggest the space group $P2_1/n$ with $a = 4.97437(11)$ Å, $b = 7.95806(15)$ Å, $c = 9.29232(19)$ Å, and $\beta = 93.8137(11)°$. The crystal structure has been solved by global optimization in direct space, using the FOX program, and refined by the Rietveld method using the FullProf program suite (see the Supporting Information, Figure S2). Hydrogen atoms were located and refined using eight restraints on bond distances (X-ray average of 0.9 Å for N–H and 1.13 Å for B–H) and fourteen restraints on bond angles. Localization of hydrogen atoms around nitrogen atoms is geometrically unambiguous because at least two heavier atoms are connected to the sp^3-hybridized pivots. The refined orientation of the −BH$_3$ group corresponds to the expected staggered configuration, further supported by the presence of two dihydrogen bonds (see the Supporting Informa-
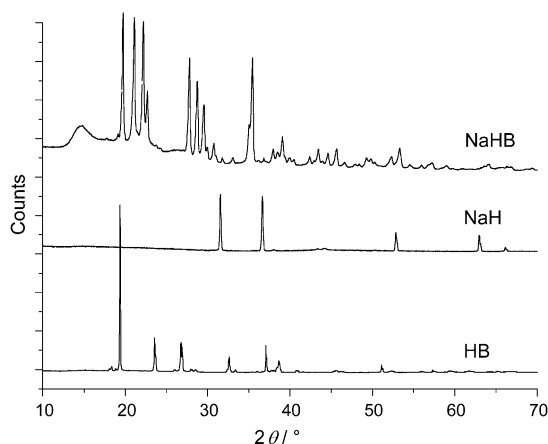
Figure 3. XRD pattern of NaHB and its comparison with patterns of the starting compounds.

tion, Figure S3). In addition, the —BH₃ group is coordinated to Na⁺ through the H···H edge, as in most other metal amidoboranes and borohydrides.[14] A common isotropic displacement factor was refined for each atom type. The final discrepancy indices are: $R_p = 1.48\%$, $R_{wp} = 2.13\%$ (not corrected for background), $R_p = 12.0\%$, $R_{wp} = 10.0\%$ (conventional), $R_B = 5.4\%$, $\chi^2 = 155$. The latter value reflects high counting statistics accumulated by the 2D detector. The reliable determination of hydrogen atom positions is highlighted by the fact that a removal of a single hydrogen atom, followed by the Rietveld refinement of all remaining parameters, cannot absorb the differences, but leads to an increase of R_B to about 7.5% and χ^2 to more than 210. Our tests show that the missing hydrogen atom can be located from difference Fourier maps typically as the highest residual peak.

The crystal structure confirms the formation of NaHB. As in the case of LiN₂H₃BH₃,[13] Na⁺ substitutes an hydrogen atom dissociated from a boron-linked nitrogen atom in the middle of the molecule. Na⁺ is surrounded by five symmetry-equivalent anions (Figure 4): four of them form a slightly distorted square environment created by two nitrogen atoms [Na—N distance is 2.396(4) and 2.428(4) Å, N—Na—N angle is 168.7(2)°] and two —BH₃ groups coordinated symmetrically through the BH₂ edges [Na···B distance is 2.947(5)–3.074(5) Å, B···Na···B angle is 140.9(2)°]. The fifth nearest neighbor completes the coordination sphere to a tetragonal pyramid, with a Na···B distance of 3.425(6) Å and a coordination through the B—H vertex. The apical distance links 2D sheets oriented in the (−101) plane in the 3D structure. The B—N distance in NaHB is 1.537(6) Å. All distances are consistent with those in the structure of NaNH₂BH₃.[15] The N—N distance is 1.453(5) Å. To sum up, XRD, IR, and NMR results confirm the successful substitution of the H^{δ+} atom in N₂H₄ by the electron-acceptor cation Na⁺[16] and the formation of NaHB.

Behavior of NaHB under heating

The behavior of NaHB under heating was analyzed by TGA (Figure 5). NaHB starts to liberate H₂ below 60°C. Concomitant-
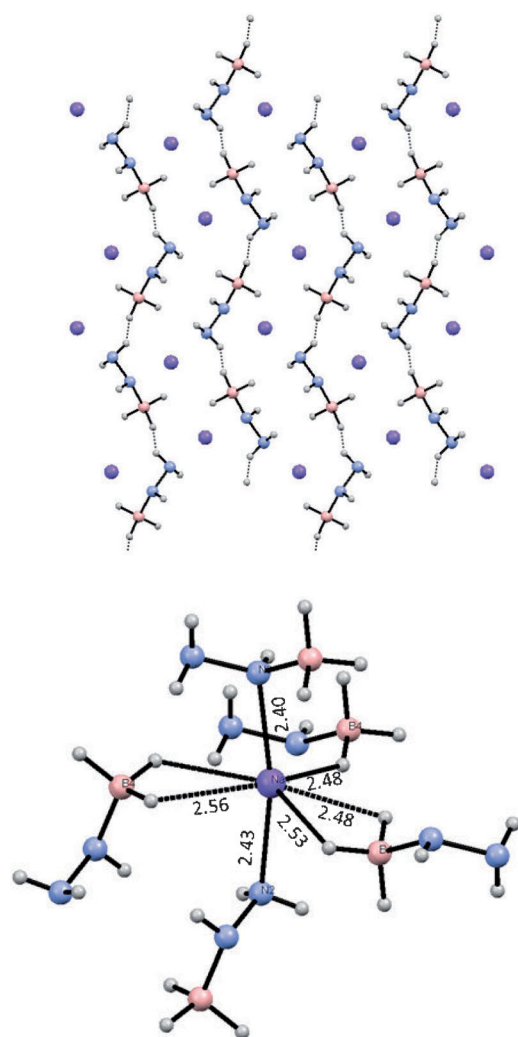
Figure 4. Crystal structure of NaN₂H₃BH₃: view (top) along the *a* axis with H···H network (dashed lines) for distances below 2.4 Å (here: 2.35 Å). The coordination sphere of Na with the distances of coordinated symmetry-equivalent anions is shown in the structure at the bottom. H, B, N, and Na atoms are represented by grey, pink, blue, and purple spheres.
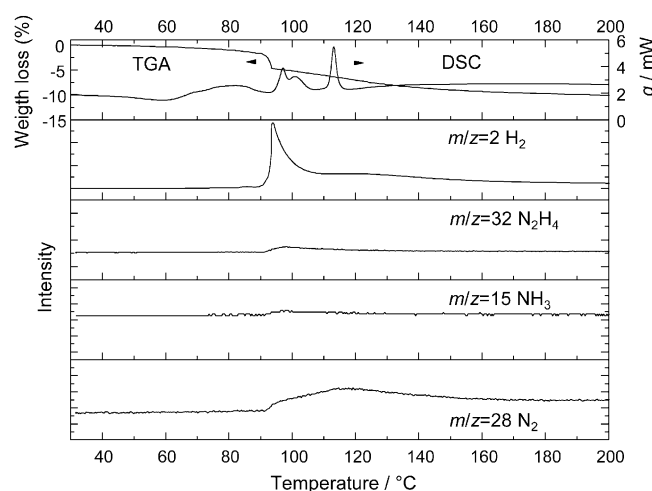
Figure 5. TGA and DSC profiles (top curves) of NaHB (heating rate of 2°C min⁻¹), and evolution of H₂ and gaseous byproducts (bottom curve) followed by MS coupled to the TGA apparatus.

ly, the solid melts. For LiN$_2$H$_3$BH$_3$, dehydrogenation starts at 70 °C.[13] Over the 60–100 °C range, NaHB loses 6 wt% of its initial weight mainly due to the loss of H$_2$, as discussed below. This is an attractive result in comparison to that obtained with pure HB (mass loss of 1.2 wt% at 95 °C),[12] or even to that obtained with neat ammonia borane (stable up to ≈ 100 °C).[9] Within 60–150 °C, NaHB dehydrogenates and the overall mass loss is 7.6 wt%. For comparison, LiN$_2$H$_3$BH$_3$ (11.69 wt%) shows a mass loss of 8.8 wt% within the temperature range of 70–150 °C.[13]

The released gases were analyzed by mass spectroscopy (Figure 5). Traces of the unwanted byproducts N$_2$H$_4$ and NH$_3$ were detected in the released hydrogen. Ammonia was also detected during the decomposition of LiN$_2$H$_3$BH$_3$.[13] The amounts of N$_2$H$_4$ liberated by NaHB are much lower than those generated by the decomposition of HB (see the Supporting Information, Figure S4). This may be attributed to the presence of Na in NaHB, with Na inhibiting the evolution of N$_2$H$_4$ and favoring the reactions between the H$^{\delta+}$ and H$^{\delta-}$ atoms. A signal at $m/z \approx 28$ could be attributed to N$_2$ (28 g mol^{-1}) and/or B$_2$H$_6$ (27.6 g mol^{-1}). IR analysis of the released gases was helpful in this identification. The spectrum (see the Supporting Information, Figure S5) shows the absence of any signal in the B—H stretching region (2000–2600 cm^{-1}), evidencing the absence of B$_2$H$_6$. The signal at $m/z \approx 28$ was thus ascribed to N$_2$, which suggests that the N$_2$H$_3^-$ moiety completely dehydrogenates. From the point of view of H$_2$ purity, the presence of N$_2$ is not problematic because it is inert towards the metal electrocatalysts used in fuel cells. This gas was also found during the decomposition of LiN$_2$H$_3$BH$_3$.[13] Notably, borazine was not detected under our experimental conditions.

The behavior of NaHB under heating was also analyzed by DSC (Figure 5). Dehydrogenation seems to be a complex reaction, consisting of four exothermic processes. These processes may be ascribed to three successive dehydrogenation stages (peaking at ≈ 75, 90, and 95 °C), followed by denitrogenation (peaking at ≈ 107 °C). The exothermic character of dehydrogenation lets us suggest that direct rehydrogenation under H$_2$ is not possible.[1,9,15]

The dehydrogenation of NaHB under prolonged heating at a constant temperature (80, 90, 95, 100, and 110 °C; Figure 6) was compared to that of HB (see the Supporting Information, Figure S6). The results obtained with HB are consistent with the results reported by Hügle et al.,[11] even though at 110 °C and within 2 h HB releases more H$_2$ in our experiments (3.7 versus 2.4 wt%). The dehydrogenation process has a two-stage profile, with the second stage having slower H$_2$ release rates. At 110 °C, the major fraction of H$_2$ (7.9 wt%) is liberated within 30 min. With respect to NaHB, the dehydrogenation profile is similar, but H$_2$ release is much faster. At 80 °C, the H$_2$ release rate is close to that found with HB, but beyond this temperature it is faster. NaHB is able to liberate 1 equiv of H$_2$ within 111 min, whereas HB releases less than 0.7 equiv of H$_2$ within the same time frame. At higher temperatures, the kinetics and extent of dehydrogenation are enhanced. The results are summarized in Table 1. For example, NaHB generates 1 equiv of H$_2$ in 5 min at 95 °C (versus 96 min for HB).
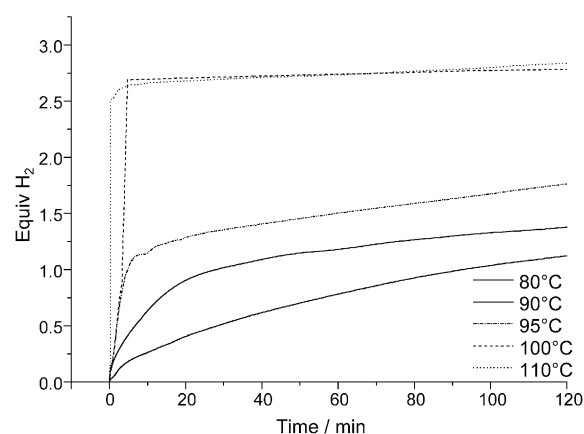
Figure 6. Dehydrogenation of NaHB under prolonged heating at five different temperatures.

Table 1. Time for the release of 1 equiv of H$_2$ from HB and NaHB with temperature increase.

T [°C]	t [min]	
	NaHB	HB
80	111	> 120
90	28	100
95	5	96
100	1	64
110	0.42	56

After heating for 2 h, about 1.1, 1.3, 1.8, 2.8, and 2.8 equiv of H$_2$ evolve at 80, 90, 95, 100, and 110 °C, respectively. Nevertheless, it is important to note that most of the H$_2$ released was generated in less than 10 min at 100 and 110 °C. That implies a material-based net effective gravimetric hydrogen-storage capacity of 3.1, 3.8, 5.2, 8.1, and 8.4 wt%, respectively. Despite the fact that different experimental conditions were used, the dehydrogenation of NaHB may be compared to that of NaNH$_2$BH$_3$ (9.45 wt%). It was reported that in 1 h the latter releases about 64% of its hydrogen content (6 wt%) under heating at about 91 °C,[15] whereas our compound liberates 50% (4.2 wt%) at 95 °C. Despite its inferior dehydrogenation performance, NaHB is a potential candidate for chemical hydrogen storage.

The gases liberated at 95 and 100 °C were analyzed by GC. At < 100 °C, H$_2$ was pure, but at > 100 °C trace amounts of NH$_3$ were detected (see the Supporting Information, Figure S7). It is noteworthy that emission of NH$_3$, but to a higher extent, was also reported in the case of NaNH$_2$BH$_3$.[17]

The dehydrogenation of NaHB at temperatures higher than 100 °C (Figure 6, Table 2) is abrupt and extremely rapid, which might be due to a different mechanism of dehydrogenation involving different reaction intermediates. At 100 and 110 °C, hydrogen-release rates (calculated for the time range necessary to liberate 2.5 equiv of H$_2$) are about 1.5 and 4 L min^{-1}. According to Gao and Shreeve,[18] the fast kinetics of H$_2$ generation might open a new perspective of energy applications (i.e, fuels in hypergolic propellant systems).

Table 2. H$_2$ release rates (r) from NaHB at various temperatures. Stages 1 and 2 refer to the dehydrogenation profile, in which two different H$_2$ release kinetics are observed. The conversion of NaHB after heating for 2 h is also provided.

T [°C]	r_1[a] [mL$_{H_2}$ min^{-1}]	r_2[a] [mL$_{H_2}$ min^{-1}]	α_{2h}[b] [%]
80	--[c]	0.1	33
90	1.3	--[d]	44
95	3.1	0.08	59
100	≈1500	0.01	91
110	≈4000	0.02	95

[a] Rate values at 100 (r_1) and 110°C (r_2) are calculated on the basis of time required to generate 2.5 equiv of H$_2$. [b] Conversion at 2 h. [c] The time of stage 1 is too short to give a relevant rate. [d] The curve is not linear, making rate difficult to determine.

Characterization of solid residues

The solid residues recovered after the heating of NaHB at 95 and 110°C for 2 h were analyzed because their identification, though often complicated,[9, 11] is important for approaching their recyclability. The XRD patterns of the residue (see the Supporting Information, Figure S8) resemble those reported in the case of heated ammonia borane, amidoboranes, or HB,[12, 15, 19] thus suggesting the formation of an amorphous polymeric phase. Nevertheless, for the sample heated at 95°C, some diffraction peaks are distinguished. Despite the fact that a thorough analysis was undertaken, we were unable to unambiguously assign XRD peaks, showing once more the difficulty to characterize the boron- and nitrogen-based solid residues. Nevertheless, the formation of NaH or Na could be eliminated. The formation of boron nitride (BN) was also ruled out by the fact that this ceramic material generally forms from boranes at temperatures much higher than 500°C.[9] Finally, a survey of the literature dedicated to boron-based materials was performed, according to which the diffraction peaks might be attributed to crystalline linear polyaminoborane (−(NH$_2$BH$_2$)$_n$−).[19]

The IR spectra (Figure 7) are typical of dehydrogenated boron-based materials.[20] The intensity of stretching bands of N−H and B−H weakened with dehydrogenation temperature. This is consistent with the increase of the degree of dehydrogenation with temperature. The intensity of the bands at 400–1300 cm^{-1} also decays. The band at 1300–1600 cm^{-1}, becoming stronger upon dehydrogenation, may be attributed to the B−N bonds in polymeric boron- and nitrogen-based compounds (e.g., polyborazylene-like).[21]

The ^{11}B MAS NMR spectrum of the residue obtained at 95°C (see the Supporting Information, Figure S9) shows a weak signal at −42.9 ppm. It corresponds to the BH$_4^-$ ion, suggesting the formation of an intermediate containing this species. For example, the formation of [(NH$_3$)$_2$BH$_2$][BH$_4$] was suggested in the thermolysis of ammonia borane.[22] A similar intermediate might tentatively be suggested as [Na$_2$(N$_2$H$_3$)$_2$BH$_2$]$^+$[BH$_4$]$^-$ in the title system. At 95°C, three [11]B resonances at positive shifts are also observed. The broader one, centered at 17.7 ppm, is assigned to three-fold boron, that is, to the BN$_3$ or N$_2$BH species, as in polyborazylene.[23] The peaks centered at
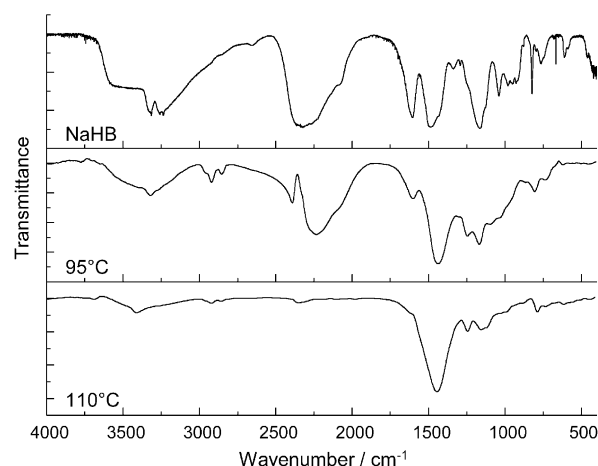
Figure 7. IR spectra of NaHB and of solid residues recovered at 95 and 110°C with: N−H stretching at 2600–3600 cm^{-1}, B−H stretching at 2000–2600 cm^{-1}, N−H bending (also B−N stretching) at 1300–1800 cm^{-1}, B−H bending at 1100–1300 cm^{-1}, N−H rocking at 900–1100 cm^{-1}, and BN−N stretching at 600–900 cm^{-1}.

1.6 and 5.9 ppm are ascribed to N$_{3-x}$BH$_x$ environments ($1 < x < 3$), typical of polycyclic boron- and nitrogen-based compounds.[24] By increasing the temperature to 110°C (see the Supporting Information, Figure S9), almost all of NaHB dehydrogenates, and BN$_3$, N$_2$BH, and N$_{3-x}$BH$_x$ species form.

The ^{23}Na MAS NMR spectrum of NaHB (see the Supporting Information, Figure S10) shows a complex signal. The signal centered at −75.7 ppm is due to a quadrupolar interaction on a single Na site in NaHB.[23] The peak at −13.6 ppm may be attributed to an amorphous phase. With the increase of temperature, the quadrupolar lineshape broadens and that gives a single resonance at −19.9 ppm at 95°C and −7.1 ppm at 110°C. This confirms the amorphization of NaHB.[23]

To sum up, the characterization of the solid residues suggests the formation of an amorphous polyborazylene-like material. Goubeau and Ricker suggested the formation of various linear and cyclic polymeric materials based on the structural units −NH$_x$−NH$_y$−BH$_z$− (with $x + y + z = 2.5$ at 95°C and 0.5 at 110°C).[4] It is assumed that Na would enter the polymeric structure because in our conditions the formation of NaH (or of Na) has not been observed.

Conclusions

We have synthesized for the first time sodium hydrazinidoborane (hydrogen content of 8.85 wt%). The results presented show that it has potential as a chemical hydrogen-storage material. A material-based gravimetric hydrogen-storage capacity slightly higher than 8 wt% is achieved with heating at 100 and 110°C. Furthermore, dehydrogenation rates were found to be high, with values of 1.5 and 4 L min^{-1}, respectively.

As in the case of the parent HB or ammonia borane and derivatives, the technological implementation of NaHB will be strongly dependent on closing the cycle of hydrogen storage. In other words, the recyclability of the spent fuel after dehydrogenation and, most importantly, the regenerability of the

borane are the key issues. The recent progress in the regeneration of ammonia borane is useful in this context.[25]

Experimental Section

Hydrazine borane (>99%) was synthesized according to a procedure described elsewhere.[12] Typically, $N_2H_4 \cdot 0.5 H_2SO_4$ (21.42 g, 264.34 mmol, Sigma–Aldrich) and $NaBH_4$ (10 g, 264.34 mmol, Acros Organics) were suspended under vigorous stirring in anhydrous dioxane (150 mL) under argon. The stirring was continued until completion of the H_2 release, which was followed by a bubble counter filled with paraffin oil. After Schlenk filtration of the mixture, dioxane was removed under vacuum. Sodium hydride (Sigma–Aldrich) was used as received. Both samples were stored in an argon-filled glove box (MBraun M200B, $H_2O < 0.1$ ppm, $O_2 < 0.1$ ppm).

NaHB was prepared by ball-milling under an argon atmosphere. In the argon-filled glove box, hydrazine borane (0.1312 g) was transferred into a stainless steel jar (25 mL). Then, stainless steel balls (ca. 20 g) were delicately and compactly aligned over the HB sample. Finally, NaH (0.0724 g) was transferred into the jar and over the balls, the ball layer acting as a barrier. The molar HB/NaH ratio was equal to 1 and the weight ratio balls/(NaH HB) was equal to 100. The transfer of NaH was performed carefully, avoiding to put both precursors into contact; this was highly important because these reactants interacted readily under ambient conditions, releasing hydrogen. Right after the NaH transfer, the closed grinding jar was carefully taken out of the glove box and placed in a vacuum flask filled with dry ice. The temperature of the jar was monitored and when it decreased to $-30\,°C$ the jar was placed in the ball mill. The milling process started immediately (250 rpm for 10 min). NaHB obtained in this way was stable under an argon atmosphere and under ambient conditions, and could be handled safely.

NaHB and the solid residues were characterized by solid-state ^{11}B MAS NMR (Varian VNMR400, ^1H 400 MHz, ^{11}B 128.37 MHz, ^{23}Na 105.86 MHZ, $-10\,°C$, 20 000 rpm), FTIR (Nicolet 710, 128 scans), thermogravimetric (Rigaku, TG8120), and DSC (DSC1 Mettler Toledo) analyses.

XRD data were collected at the Swiss–Norwegian Beam Lines at the ESRF research institute by means of the Pilatus 2M detector using a wavelength of 0.69412 Å. Indexing was performed using the DICVOL04 program.[26] The structure was solved by parallel tempering in FOX,[27] and refined by the Rietveld method with the FullProf suite.[28] The structure shown in Figure 4 fitted the diffraction pattern well (see the Supporting Information, Figure S2) with an agreement factor (R_{wp}) of 10.0% and a Bragg R-factor (R_B) of 5.4%.

The dehydrogenation of NaHB under prolonged heating at constant temperatures (80, 90, 85, 100, and 110 °C) was performed on our thermolysis bench. A flask was linked to a Schlenk line and was immersed in an oil bath heated to the desired temperature. The outlet of the flask was connected to an inverted burette filled with colored water through a cold trap maintained at 0 °C. The whole bench was maintained under a N_2 atmosphere. The H_2 evolution was video-recorded and the data plotted using the Matlab software.

The purity of H_2 was analyzed by mass spectrometry (Anelva, M-QA200TS) coupled to the TGA apparatus and by GC analysis (Shimadzu, GC-14B). The gases collected in a Tedlar bag were also analyzed by FTIR (Nicolet Nexus, high-resolution detector MCT/A, 1024 scans, resolution of 0.1 cm^{-1}).

[1] a) L. Schlapbach, A. Züttel, *Nature* **2001**, *414*, 353–358; b) W. Grochala, P. P. Edwards, *Chem. Rev.* **2004**, *104*, 1283–1316; c) U. Eberle, M. Felderhoff, F. Schüth, *Angew. Chem.* **2009**, *121*, 6732–6757; *Angew. Chem. Int. Ed.* **2009**, *48*, 6608–6630; d) J. Graetz, *Chem. Soc. Rev.* **2009**, *38*, 73–82; e) J. Yang, A. Sudik, C. Wolverton, D. J. Siegel, *Chem. Soc. Rev.* **2010**, *39*, 656–675; f) P. E. de Jongh, P. Adelhelm, *ChemSusChem* **2010**, *3*, 1332–1348; g) N. Armaroli, V. Balzani, *ChemSusChem* **2011**, *4*, 21–36; h) H. Reardon, J. M. Hanlon, R. W. Hugues, A. Godula-Jopek, T. K. Mandal, D. H. Gregory, *Energy Environ. Sci.* **2012**, *5*, 5951–5979.

[2] N. Vinh-Son, S. Swinnen, M. H. Matus, M. T. Nguyen, D. A. Dixon, *Phys. Chem. Chem. Phys.* **2009**, *11*, 6339–6344.

[3] a) R. von Helmolt, U. Eberle, *J. Power Sources* **2007**, *165*, 833–843; b) U. B. Demirci, P. Miele, *Energy Environ. Sci.* **2011**, *4*, 3334–3341.

[4] V. J. Goubeau, E. Ricker, *Z. Anorg. Allg. Chem.* **1961**, *310*, 123–142.

[5] S. Karahan, M. Zahmakıran, S. Özkar, *Int. J. Hydrogen Energy* **2011**, *36*, 4958–4966.

[6] *Targets for Onboard Hydrogen Storage Systems for Light-Duty Vehicles*, US Department of Energy, Office of Energy Efficiency and Renewable Energy and The FreedomCAR and Fuel Partnership, **2009**. Available at http://www1.eere.energy.gov/hydrogenandfuelcells/storage/pdfs/targets_onboard_hydro_storage_explanation.pdf.

[7] a) M. G. Hu, R. A. Geanangel, W. W. Wendlandt, *Thermochim. Acta* **1978**, *23*, 249–255; b) V. Sit, R. A. Geanangel, W. W. Wendlandt, *Thermochim. Acta* **1987**, *113*, 379–382.

[8] a) G. Wolf, J. Baumann, F. Baitalow, F. P. Hoffmann, *Thermochim. Acta* **2000**, *343*, 19–25; b) F. Baitalow, J. Baumann, G. Wolf, K. Jaenicke-Rößler, G. Leitner, *Thermochim. Acta* **2002**, *391*, 159–168; c) F. Baitalow, G. Wolf, J. P. E. Grolier, F. Dan, S. L. Randzio, *Thermochim. Acta* **2006**, *445*, 121–125; d) J. Baumann, F. Baitalow, *Thermochim. Acta* **2005**, *430*, 9–14.

[9] a) C. W. Hamilton, R. T. Baker, A. Staubitz, I. Manners, *Chem. Soc. Rev.* **2009**, *38*, 279–293; b) U. Sanyal, U. B. Demirci, B. R. Jagirdar, P. Miele, *ChemSusChem* **2011**, *4*, 1731–1739; c) H. L. Jiang, S. K. Singh, J. M. Yan, X. B. Zhang, Q. Xu, *ChemSusChem* **2010**, *3*, 541–549.

[10] J. Hannauer, O. Akdim, U. B. Demirci, C. Geantet, J. M. Herrmann, P. Miele, Q. Xu, *Energy Environ. Sci.* **2011**, *4*, 3355–3358.

[11] T. Hügle, M. F. Kühnel, D. Lentz, *J. Am. Chem. Soc.* **2009**, *131*, 7444–7446.

[12] R. Moury, G. Moussa, U. B. Demirci, J. Hannauer, S. Bernard, E. Petit, A. van der Lee, P. Miele, *Phys. Chem. Chem. Phys.* **2012**, *14*, 1768–1777.

[13] H. Wu, W. Zhou, F. E. Pinkerton, T. J. Udovic, T. Yildirim, J. J. Rush, *Energy Environ. Sci.* **2012**, *5*, 7531–7535.

[14] Y. Filinchuk, D. Chernyshov, V. Dmitriev, *Z. Kristallogr.* **2008**, *223*, 649–659.

[15] a) Z. Xiong, C. K. Yong, G. Wu, P. Chen, W. Shaw, A. Karkamkar, T. Autrey, M. O. Jones, S. R. Johnson, P. P. Edwards, W. I. F. David, *Nat. Mater.* **2008**, *7*, 138–141; b) S. Chua, W. Li, W. J. Shaw, G. Wu, T. Autrey, Z. Xiong, M. W. Wong, P. Chen, *ChemSusChem* **2012**, *5*, 927–931.

[16] Y. S. Chua, G. T. Wu, Z. T. Xiong, T. He, P. Chen, *Chem. Mater.* **2009**, *21*, 4899–4904.

[17] K. J. Fijałkowski, W. Grochala, *J. Mater. Chem*. **2009**, *19*, 2043–2050.

[18] H. Gao, J. M. Shreeve, *J. Mater. Chem.* **2012**, *22*, 11022–11027.

[19] T. He, J. Wang, G. Wu, H. Kim, T. Proffen, A. Wu, W. Li, T. Liu, Z. Xiong, C. Wu, H. Chu, J. Guo, T. Autrey, T. Zhang, P. Chen, *Chem. Eur. J.* **2010**, *16*, 12814–12817.

[20] U. B. Demirci, S. Bernard, R. Chiriac, F. Toche, P. Miele, *J. Power Sources* **2011**, *196*, 279–286.

[21] P. J. Fazen, E. E. Remsen, J. S. Beck, P. J. Carroll, A. R. McGhie, L. G. Sneddon, *Chem. Mater.* **1995**, *7*, 1942–1956.

[22] A. C. Stowe, W. J. Shaw, J. C. Linehan, B. Schmid, T. Autrey, *Phys. Chem. Chem. Phys.* **2007**, *9*, 1831–1836.

[23] K. Shimoda, Y. Zhang, T. Ichikawa, H. Miyaoka, Y. Kojima, *J. Mater. Chem.* **2011**, *21*, 2609–2615.

[24] D. Neiner, A. Karkamkar, J. C. Linehan, B. Arey, T. Autrey, S. M. Kauzlarich, *J. Phys. Chem. C* **2009**, *113*, 1098–1103.

[25] a) B. L. Davis, D. A. Dixon, E. B. Garner, J. C. Gordon, M. H. Matus, B. Scott, F. H. Stephens, *Angew. Chem.* **2009**, *121*, 6944–6948; *Angew. Chem. Int. Ed.* **2009**, *48*, 6812–6816; b) A. Sutton, A. K. Burrell, D. A. Dixon, E. B. Garner, III., J. C. Gordon, T. Nakagawa, K. C. Ott, J. P. Robinson, M. Vasiliu, *Science* **2011**, *331*, 1426–1429.

[26] a) T. Roisnel, J. Rodríguez-Carvajal, WinPLOTR, Proceedings of the Seventh European Powder Diffraction Conference (EPDIC 7), (Ed.: R. Delhez, E. J. Mittenmeijer), **2000**, 118–123; b) A. Boultif, D. Louer, *J. Appl. Crystallogr.* **2004**, *37*, 724–731.

[27] V. Favre-Nicolin, R. Cerny, *J. Appl. Crystallogr.* **2002**, *35*, 734–743.

[28] J. Rodríguez-Carvajal, *Physica B* **1993**, *192*, 55–69.